FEATURE ARTICLE

Solvation Dynamics in Electron-Transfer, Isomerization, and Nonlinear Optical Processes. A Unified Liouville-Space Theory

Yi Jing Yan, Massimo Sparpaglione,[†] and Shaul Mukamel*[,‡]

Department of Chemistry, University of Rochester, Rochester, New York 14627 *(Received: January 6, 1988)*

A correlation function formulation, based on the Liouville equation for the density matrix, provides a microscopic theory for solvation dynamics and establishes a general fundamental connection between the calculation of rate processes and nonlinear optical processes in solution. The present rate theory requires the calculation of four-point correlation functions of the nonadiabatic coupling, which is formally identical with the calculation of four-wave-mixing processes and the nonlinear susceptibility $\chi^{(3)}$. A novel semiclassical propagation scheme (the Liouville-space generating function, LGF) is developed and used in these calculations. The connection with $\chi^{(3)}$ may allow the direct use of solvent correlation functions obtained from nonlinear optical measurements, in the calculation of molecular rate processes. The present theory interpolates continuously from the adiabatic to the nonadiabatic limits. A new criterion for adiabaticity is derived, and the role of the solvent time scale in inducing the crossover from the nonadiabatic to the adiabatic regimes is clarified. The present results generalize the Kramers theory of isomerization and the Marcus theory of electron transfer in polar solvents. Both static (polarity) interactions, which affect the reaction energetics and dynamic (friction) effects, are properly incorporated.

I. Introduction

The dynamics of solvation plays an essential role in controlling rate processes as well as the optical properties of molecular systems.[1-4] The limiting step in electron-transfer (ET) processes[5-18] is a proper dielectric fluctuation which compensates for the activation energy and allows the ET to proceed. Isomerization reactions in condensed phases are strongly affected by the friction originating from the interaction with the solvent.[19-30] Similarly, the optical properties of solvated molecular systems are often dominated by the dephasing processes induced by the solvent,[4,31-37] which result in spectral shifts and line broadening. Recent developments in laser spectroscopy provide a broad range of frequency-domain and time-domain linear and nonlinear optical techniques with femtosecond resolution.[31-37] Many of the most widely used nonlinear techniques are some form of four-wave mixing (4WM). Transient grating, coherent anti-Stokes Raman (CARS), hole-burning, and photon echo spectroscopies, degenerate four-wave mixing, and the Kerr effect are just a few examples of 4WM. A calculation of any 4WM process requires the evaluation of a four-time correlation function of the dipole operator.[38] In recent years, we have developed a systematic methodology for relating a variety of 4WM observables to the same four-point correlation function.[38-42] Various stochastic and microscopic models were then developed and applied toward the calculation of the four-point correlation function. We have further shown how spontaneous Raman and fluorescence can also be treated in the same way.[42,43] Rate processes in condensed phases are commonly treated by using stochastic methods.[1,2] The Marcus theory for ET uses a dielectric continuum model for the solvent.[5] Isomerization reactions are often treated by means of the Kramers theory,[44,45] which is based on a Langevin equation.[28,29] We have further shown how the dynamics of rate processes can be related to the same four-point correlation functions which appear in 4WM.[46] This provides an important and fundamental link between the dynamics of rate processes and nonlinear optical measurements. It allows us to clarify the precise information content of nonlinear spectroscopy and how it can be directly utilized to predict rate processes. In this article, we review these recent developments and discuss the connection between rate

[†] Current address: Enichem R&D, Via Medici del Vascello 26, Milano 20138, Italy.
[‡] Camille and Henry Dreyfus Teacher-Scholar.

(1) See: *J. Phys. Chem.* **1986**, *90* (special issue honoring R. A. Marcus).
(2) See: *J. Stat. Phys.* **1986**, *42* ("Proceedings of the Symposium on Rate Processes and First Passage Times").
(3) *The Chemical Physics of Solvation*; Dogonadze, R. R., Kalman, E., Kornyshev, A. A., Ulstrup, J., Eds.; Elsevier: Amsterdam, 1985.
(4) Fleming, G. R. *Chemical Applications of Ultrafast Spectroscopy*; Oxford: London, 1986.
(5) Marcus, R. A. *J. Chem. Phys.* **1965**, *43*, 679. For reviews see: Marcus, R. A. *Annu. Rev. Phys. Chem.* **1964**, *15*, 155. Marcus, R. A.; Sutin, N. *Biochim. Biophys. Acta* **1985**, *811*, 265.
(6) (a) Kosower, E.; Huppert, D. *Chem. Phys. Lett.* **1983**, *96*, 423. (b) Kosower, E. *Annu. Rev. Phys. Chem.* **1986**, *37*, 127.
(7) Miller, J. R.; Calcaterra, L. T.; Closs, G. L. *J. Am. Chem. Soc.* **1984**, *106*, 304.
(8) Heisel, F.; Miehe, J. A. *Chem. Phys.* **1985**, *98*, 23. Heisel, F.; Miehe, J. A.; Martinho, J. M. G. *Chem. Phys.* **1985**, *98*, 263.
(9) Makinen, M. W.; Schichman, S. A.; Hill, S. C.; Gray, H. B. *Science* **1983**, *222*, 929.
(10) McGuire, M.; McLendon, G. *J. Phys. Chem.* **1986**, *90*, 2549.
(11) Schmidt, J. A.; Siemiarczuk, A.; Weedon, A. C.; Bolton, J. R. *J. Am. Chem. Soc.* **1985**, *107*, 6112. Schmidt, J. A.; Liu, J. Y.; Bolton, J. R.; Archer, M. D.; Gadzekpo, V. P. Y. *J. Am. Chem. Soc.*, in press.
(12) Zusman, L. D. *Chem. Phys.* **1980**, *49*, 295; *Chem.* Phys. **1983**, *80*, 29. Zusman, L. D.; Helman, A. B. *Opt. Spec. (USSR)* **1982**, *53*, 248. Zusman, L. D.; Helman, A. B. *Chem. Phys.* **1985**, *114*, 301.
(13) Newton, M.; Sutin, N. *Am. Rev. Phys. Chem.* **1984**, *35*, 937.
(14) Sumi, H.; Marcus, R. A. *J. Chem. Phys.* **1986**, *84*, 4272, 4894.
(15) Chandler, D. *J. Stat. Phys.* **1986**, *42*, 49. See also the works related to isomerization: Chandler, D. *J. Chem. Phys.* **1978**, *68*, 2959. Montgomery, J.; Chandler, D.; Berne, B. J. *J. Chem. Phys.* **1979**, *70*, 4056.
(16) Frauenfelder, H.; Wolynes, P. G. *Science* **1985**, *229*, 337.
(17) Rips, I.; Jortner, J. *Chem. Phys. Lett.* **1987**, *133*, 411; *J. Chem. Phys.* **1987**, *87*, 2090.
(18) Newton, M. D.; Friedman, H. L. *J. Chem. Phys.* **1988**, *88*, 4460.
(19) (a) Millar, D. P.; Eisenthal, K. B. *J. Chem. Phys.* **1985**, *83*, 5076. (b) Hicks, J.; Vandersoll, M.; Barbarogic, Z.; Eisenthal, K. B. *Chem. Phys. Lett.* **1985**, *116*, 18. (c) Hicks, J.; Vandersoll, M.; Sitzmann, E. V.; Eisenthal, K. B. *Chem. Phys. Lett.* **1987**, *135*, 413.
(20) Velsko, S. P.; Waldeck, D. H.; Fleming, G. R. *J. Chem. Phys.* **1983**, *78*, 294. Waldeck, D.; Fleming, G. R. *J. Phys. Chem.* **1981**, *85*, 2614. Velsko, S. P.; Fleming, G. R. *J. Chem. Phys.* **1987**, *76*, 3553.
(21) Schroeder, J.; Troe, J. *Chem. Phys. Lett.* **1985**, *116*, 453. Maneke, G.; Schroeder, J.; Troe, J.; Voss, F. *Ber. Bunsen-Ges. Phys. Chem.* **1985**, *89*, 986. Troe, J. *Chem. Phys. Lett.* **1985**, *114*, 241.
(22) Lee, M.; Bain, A. J.; McCarthy, P. J.; Ham, C. H.; Haseltine, J. N.; Smith III, A. B.; Hochstrasser, R. M. *J. Chem. Phys.* **1986**, *85*, 4341.
(23) Syage, J.; Felker, P.; Zewail, A. *J. Chem. Phys.* **1986**, *81*, 4685; **1984**, *81*, 4706.

0022-3654/88/2092-4842$01.50/0

theories and nonlinear optical line shapes.

In section II we define the linear and the nonlinear response functions ($J(t_1)$ and $R(t_3,t_2,t_1)$, respectively) and show how four-wave-mixing ($\chi^{(3)}$) measurements as well as rate processes may be expressed in terms of these quantities. In section III, we develop a specific model of a damped harmonic coordinate coupled to the electronic transition and derive explicit expressions for the response functions and for isomerization rates. These expressions assume a particularly simple form when the static (high-temperature) limit holds. In section IV, we show how the expressions derived in section III may be applied to electron transfer in polar solvents. The solvation dynamics are expressed, in this case, in terms of the dielectric properties of the solvent. In section V we consider the special case where the solvation coordinate has an exponential correlation function $\exp(-\Lambda t)$. This model applies for isomerization in the Smoluchowski limit, for electron transfer in Debye solvents, and for spectral line broadening when the molecular frequency undergoes a stochastic Gaussian–Markovian process. For this case, a more general expression for the rate, not restricted to the static limit, may be derived. In section VI we present numerical calculations of electron-transfer rates and time- and frequency-resolved fluorescence and hole-burning line shapes in polar solvents. Finally, we summarize and discuss our results in section VII.

II. The Nonlinear Response Function: A Unified Description of Nonlinear Spectroscopy and Rate Processes

We start our analysis by considering a spectroscopic experiment involving a molecular system with two electronic levels ($|a\rangle$ and $|b\rangle$) in a solvent. The total Hamiltonian is

$$H_T = H + H_{int} \tag{II-1}$$

where the molecular Hamiltonian is

$$H = |a\rangle H_a \langle a| + |b\rangle H_b \langle b| \tag{II-2}$$

and H_{int} represents the interaction with the electromagnetic field

$$H_{int} = -\mu E(\mathbf{r},t)(|a\rangle\langle b| + |b\rangle\langle a|) \tag{II-3}$$

Here H_a and H_b represent the Hamiltonians for the intramolecular (vibration, rotation) and for the solvent degrees of freedom, when the system is in the electronic states $|a\rangle$ and $|b\rangle$, respectively. μ is the electronic transition dipole matrix element. We shall treat the electromagnetic field classically and decompose it into Fourier components:

$$E(\mathbf{r},t) = \sum_j E_j(t) \exp(i\mathbf{k}_j\mathbf{r} - i\omega_j t) + \text{C.C.} \tag{II-4}$$

The optical properties of the system may be related to the wavevector and time-dependent polarization $P(\mathbf{k},t)$. The polarization is usually expanded in a Taylor series in E:[31,38]

$$P(\mathbf{k},t) = P^{(1)}(\mathbf{k},t) + P^{(2)}(\mathbf{k},t) + P^{(3)}(\mathbf{k},t) + \ldots \tag{II-5}$$

$P^{(1)}$ is related to the linear optical properties, whereas $P^{(2)}$, $P^{(3)}$, etc., constitute nonlinear contributions. In an isotropic medium $P^{(2)} = 0$. In this article, we shall focus on $P^{(1)}$ and $P^{(3)}$.

To first order we consider a single field E_1, and we have

$$P^{(1)}(\mathbf{k}_1,t) = i|\mu|^2 \int_0^\infty dt_1\ [J(t_1) - J^*(t_1)] \exp(i\omega_1 t_1) E_1(t-t_1) \tag{II-6}$$

where $[J(t_1) - J^*(t_1)]$ is the *linear response function*. Turning now to $P^{(3)}$, we assume that the incoming field has three Fourier components, $j = 1, 2, 3$. The resulting polarization can have any of the wavevectors $\pm\mathbf{k}_1$, $\pm\mathbf{k}_2$, $\pm\mathbf{k}_3$ and the corresponding frequencies $\pm\omega_1$, $\pm\omega_2$, $\pm\omega_3$. We shall hereafter calculate the following component of the polarization

$$\mathbf{k}_s = \mathbf{k}_1 + \mathbf{k}_2 + \mathbf{k}_3 \tag{II-7a}$$

$$\omega_s = \omega_1 + \omega_2 + \omega_3 \tag{II-7b}$$

It is given by

$$P^{(3)}(\mathbf{k}_s,t) = i^3|\mu|^4 \sum \int_0^\infty dt_1 \int_0^\infty dt_2 \int_0^\infty dt_3\ [R(t_3,t_2,t_1) - R^*(t_3,t_2,t_1)] E_1(t-t_1-t_2-t_3)\ E_2(t-t_2-t_3)\ E_3(t-t_3) \times \exp[i(\omega_1+\omega_2+\omega_3)t_3 + i(\omega_1+\omega_2)t_2 + i\omega_1 t_1] \tag{II-8}$$

The summation in eq II-8 implies that we have to sum over all the permutations of E_1, E_2, E_3 (and ω_1, ω_2, ω_3). Other Fourier components of $P^{(3)}$ may be obtained from eq II-8 by changing the sign of one (or more) ω_j to $-\omega_j$ and E_j to E_j^*. $[R(t_3,t_2,t_1) - R^*(t_3,t_2,t_1)]$ is the third-order *nonlinear response function*. Equations II-6 and II-8 allow for an arbitrary temporal profile of $E_j(t)$ and are valid for pulsed as well as steady-state experiments. In a steady-state experiment we take $E_j(t) = E_j$ independent of time. We can then factorize E_j out of the integrations, and eq II-6 and II-8 may be recast in the form

$$P^{(1)}(\mathbf{k}_1,t) = \chi^{(1)}(-\omega_1;\omega_1)E_1 \tag{II-9a}$$

$$P^{(3)}(\mathbf{k}_s,t) = \chi^{(3)}(-\omega_s;\omega_1,\omega_2,\omega_3)E_1,E_2,E_3 \tag{II-9b}$$

$\chi^{(1)}$ and $\chi^{(3)}$ are the first- and the third-order *optical susceptibilities*, respectively.[31,38]

The functions $J(t_1)$ and $R(t_3,t_2,t_1)$ may be calculated starting with the Hamiltonian and with the Liouville equation for the density matrix of the system

$$d\hat{\rho}/dt = -i[H,\hat{\rho}] - i[H_{int},\hat{\rho}] \tag{II-10a}$$

(24) Amirav, A.; Jortner, J. *Chem. Phys. Lett.* **1983**, *95*, 295. Majors, T. J.; Even, U.; Jortner, J. *J. Chem. Phys.* **1984**, *81*, 2330.

(25) Amotz, D. Ben; Harris, C. C. *J. Chem. Phys.* **1987**, *86*, 4856, 5433. Amotz, D. Ben; Jeanlox, R.; Harris, C. B. *J. Chem. Phys.* **1987**, *86*, 6119.

(26) Su, S. G.; Simon, J. D. *J. Phys. Chem.* **1987**, *91*, 2693.

(27) Barbara, P. F.; Jarzeka, P. *Acc. Chem. Res.* **1988**, *21*, 195. Kahlow, M. A.; Kang, T. G.; Barbara, P. F. *J. Chem. Phys.* **1988**, *88*, 2372.

(28) (a) Grote, R. F.; Hynes, J. T. *J. Chem. Phys.* **1980**, *73*, 2715. (b) Hynes, J. T. *J. Phys. Chem.* **1986**, *90*, 3701. (c) Hynes, J. T. *Annu. Rev. Phys. Chem.* **1985**, *36*, 573.

(29) Straub, J. E.; Borkovec, M.; Berne, B. J. *J. Chem. Phys.* **1986**, *86*, 1788.

(30) (a) Bagchi, B.; Fleming, G. R.; Oxtoby, D. W. *J. Chem. Phys.* **1983**, *78*, 7375. (b) Bagchi, B.; Oxtoby, D. *J. Chem. Phys.* **1982**, *77*, 1391.

(31) Shen, Y. R. *The Principles of Nonlinear Optics*; Wiley: New York, 1984.

(32) Fayer, M. D. *Annu. Rev. Phys. Chem.* **1982**, *33*, 63.

(33) Laubereau, A.; Kaiser, W. *Rev. Mod. Phys.* **1978**, *50*, 607.

(34) Small, G. J. In *Spectroscopy and Excitation Dynamics of Condensed Molecular Systems*; Agranovich, V. M., Hochstrasser, R. H., Eds.; North-Holland: New York, 1983; p 515. Caau, T. C.; Johnson, C. K.; Small, G. J. *J. Phys. Chem.* **1985**, *89*, 2984. Small, G. J. In *Modern Problems in Condensed Matter Sciences*; Agranovich, V. M., Maradudin, A. A., Eds.; North-Holland: Amsterdam, 1983; Vol. 4.

(35) *Ultrafast Phenomena V*; Fleming, G. R., Siegman, A. E., Eds.; Springer-Verlag: Berlin, 1986.

(36) Migus, A.; Gauduel, Y.; Martin, J. L.; Antonetti, A. *Phys. Rev. Lett.* **1987**, *58*, 1559.

(37) (a) Castner, E. W.; Maroncelli, M.; Fleming, G. R. *J. Chem. Phys.* **1987**, *86*, 1090. Maroncelli, M.; Fleming, G. R. *J. Chem. Phys.* **1987**, *86*, 6221. (b) Shank, C. V.; Fork, R. L.; Brito Cruz, C. H.; Knox, W. In *Ultrafast Phenomena V*; Fleming, G. R., Siegman, A. E., Eds.; Springer: Berlin, 1986. Brito Cruz, C. H.; Fork, R. L.; Knox, W.; Shank, C. V. *Chem. Phys. Lett.* **1986**, *132*, 341.

(38) Mukamel, S. *Phys. Rev. A* **1983**, *28*, 3480. Mukamel, S.; Loring, R. F. *J. Opt. Soc. Am. B: Opt. Phys.* **1986**, *3*, 595.

(39) Mukamel, S. *J. Chem. Phys.* **1979**, *71*, 2884; **1982**, *77*, 173.

(40) Mukamel, S. *Phys. Rep.* **1982**, *93*, 1; *J. Phys. Chem.* **1984**, *88*, 3185; *Adv. Chem. Phys.* **1988**, *70* (Part I), 165.

(41) Loring, R. F.; Mukamel, S. *J. Chem. Phys.* **1985**, *83*, 2116.

(42) Loring, R. F.; Yan, Y. J.; Mukamel, S. *J. Chem. Phys.* **1987**, *87*, 5840.

(43) Sue, J.; Yan, Y. J.; Mukamel, S. *J. Chem. Phys.* **1986**, *85*, 462. Yan, Y. J.; Mukamel, S. *J. Chem. Phys.* **1986**, *85*, 5908; **1987**, *86*, 6085.

(44) Kramers, H. A. *Physica (Amsterdam)* **1940**, *7*, 284.

(45) Risken, H. *The Fokker-Planck Equation*; Springer-Verlag: Berlin, 1984.

(46) Sparpaglione, M.; Mukamel, S. *J. Chem. Phys.* **1988**, *88*, 3263, 4300; *J. Phys. Chem.* **1987**, *91*, 3938.

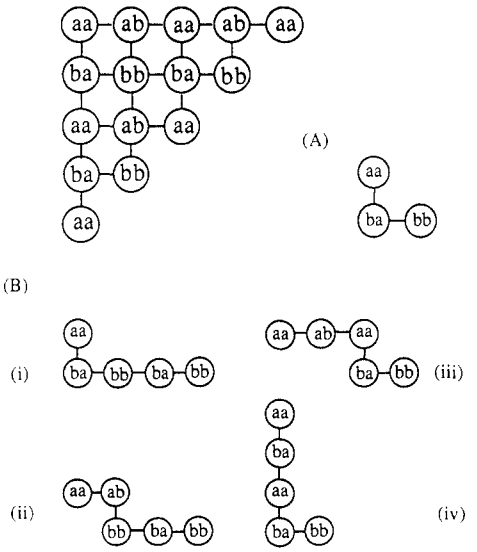

Figure 1. The Liouville-space coupling scheme and the four pathways contributing to the nonlinear response function.[38] Solid lines denote the interaction H_{int}. Horizontal (vertical) lines represent action of H_{int} from the right (left). Starting with aa in the upper left corner, there are two and eight pathways which lead to bb in second and in fourth order, respectively. Only half of these pathways are shown. The contribution of the other pathways is the complex conjugate of those shown. The pathway labeled (A) contributes to the linear response function $J(t_1)$ (eq II-11). The four pathways labeled (B) [(i), (ii), (iii), and (iv)] correspond respectively to R_1, R_2, R_3, and R_4 of eq II-13 and contribute to the nonlinear response function.

Equation II-10a is then solved perturbatively in H_{int}, assuming that initially the system is in thermal equilibrium within the $|a\rangle$ state, i.e.

$$\hat{\rho}(0) = \rho_a \equiv \exp(-H_a/kT)/\mathrm{Tr}\,\exp(-H_a/kT) \qquad \text{(II-10b)}$$

The polarization is calculated by taking the expectation value of the dipole operator $\hat{\mu}$, after $\hat{\rho}$ is calculated to the desired order (first order for J, third order for R). Within the Condon approximation, the linear response function is then given by

$$J(t_1) = \langle G_{ba}(t_1)\rho_a\rangle \qquad \text{(II-11)}$$

and the nonlinear response function assumes the form

$$R(t_3,t_2,t_1) = \sum_{\alpha=1}^{4} R_\alpha(t_3,t_2,t_1) \qquad \text{(II-12)}$$

$$R_1(t_3,t_2,t_1) = \langle G_{ba}(t_3)\, G_{bb}(t_2)\, G_{ba}(t_1)\rho_a\rangle \qquad \text{(II-13a)}$$

$$R_2(t_3,t_2,t_1) = \langle G_{ba}(t_3)\, G_{bb}(t_2)\, G_{ab}(t_1)\rho_a\rangle \qquad \text{(II-13b)}$$

$$R_3(t_3,t_2,t_1) = \langle G_{ba}(t_3)\, G_{aa}(t_2)\, G_{ab}(t_1)\rho_a\rangle \qquad \text{(II-13c)}$$

$$R_4(t_3,t_2,t_1) = \langle G_{ba}(t_3)\, G_{aa}(t_2)\, G_{ba}(t_1)\rho_a\rangle \qquad \text{(II-13d)}$$

$G_{mn}(t)$ is a Liouville-space Green function,[40] defined by its action on an arbitrary operator A

$$G_{mn}(t)A \equiv \exp(-iH_m t)A\,\exp(iH_n t) \qquad \text{m, n = a, b} \qquad \text{(II-14)}$$

The Liouville-space pathways corresponding to eq II-13 are displayed in Figure 1. Initially, the system is in the $|a\rangle$ state (and the density matrix is $|a\rangle\langle a|$). This is represented by the aa in the upper left corner of Figure 1. In the Liouville equation (II-10a), H_{int} appears in a commutator, and each time it is applied, it can act either from the left or from the right. In Figure 1, a vertical (horizontal) line represents the action of H_{int} from the left (right). After one action of H_{int} from the left, the system moves one step down to $|b\rangle\langle a|$ (ba), whereas after one action of H_{int} from the right the system moves one step to the right to $|a\rangle\langle b|$ (ab). The density matrix to first order, or to third order, in H_{int} is calculated by acting with H_{int} once, or three times, respectively. Finally, we calculate the polarization by acting with the dipole operator from the right and calculating the trace. In fact, the last interaction can be applied either from the left or from the right. In previous calculations of the nonlinear polarization we have applied the last interaction from the left.[40] The connection with rate processes is somewhat more transparent if we apply the last interaction from the right. This is why we make this choice in this article. Let us first consider the linear polarization. There are two distinct pathways in Liouville space for the first H_{int} interaction. However, only one of the pathways is independent. The pathway is displayed in Figure 1A and corresponds to the calculation of the function $J(t_1)$ (eq II-11). The other pathway is simply the complex conjugate and corresponds to $J^*(t_1)$. We now consider the third-order nonlinear polarization. There are $2^3 = 8$ distinct pathways in Liouville space corresponding to the possible choices of "left" and "right" for the three H_{int} interactions. However, only four of these pathways are independent; the other four are simply their complex conjugate. We thus need to consider only the four pathways (i), (ii), (iii), and (iv) displayed in Figure 1B, which correspond to R_1, R_2, R_3, and R_4 (eq II-13), respectively.

We have developed a Liouville-space semiclassical propagation scheme for evaluating eq II-11 and II-13.[47-49] The method is based on propagating a *Liouville-space generating function* (LGF) $\rho(t)$ defined as follows:

$$\rho(0) = \rho_a \equiv \exp(-H_a/kT)/\mathrm{Tr}\,\exp(-H_a/kT) \qquad \text{(II-15a)}$$

$$\rho(t_1) \equiv G_{mn}(t_1)\rho_a = \exp(-iH_m t_1)\rho_a\,\exp(iH_n t_1) \qquad \text{(II-15b)}$$

$$\rho(t_1+t_2) \equiv G_{ll}(t_2)\,\rho(t_1) = \exp(-iH_l t_2)\,\rho(t_1)\,\exp(iH_l t_2) \qquad \text{(II-15c)}$$

$$\rho(t_1+t_2+t_3) \equiv G_{jk}(t_3)\,\rho(t_1+t_2) = \exp(-iH_j t_3)\,\rho(t_1+t_2)\,\exp(iH_k t_3) \qquad \text{(II-15d)}$$

The linear response function can be calculated by

$$\langle G_{mn}(t_1)\rho_a\rangle \equiv \mathrm{Tr}\,\rho(t_1) \qquad \text{(II-16)}$$

whereas the nonlinear response function requires the evaluation of

$$\langle G_{jk}(t_3)\, G_{ll}(t_2)\, G_{mn}(t_1)\rho_a\rangle \equiv \mathrm{Tr}\,\rho(t_1+t_2+t_3) \qquad \text{(II-17)}$$

The calculation of $J(t_1)$ (eq II-11) thus requires starting with ρ_a and performing a propagation for one time interval (t_1) with the choice m = b and n = a, resulting in $\rho(t_1)$. The trace of $\rho(t_1)$ will then yield $J(t_1)$. The calculation of the nonlinear response function requires propagating ρ for three time intervals t_1, t_2, and t_3 successively and then performing a trace. It should be noted that the LGF $\rho(t)$ is not the density matrix of the system, since its propagation from the left and from the right is with different Hamiltonians. In eq II-15b, for example, $\rho(t)$ evolves in time following H_m from the left and H_n from the right. $\rho(t_1+t_2+t_3)$ denotes a Liouville-space generating function at time $t_1 + t_2 + t_3$. *This function depends on all three time arguments t_1, t_2, and t_3, and not only on $t_1 + t_2 + t_3$.* The reason is that in each time interval there is a different propagation (i.e., $G_{mn}(t_1)$, $G_{ll}(t_2)$, and $G_{jk}(t_3)$). Consequently, the functions $\rho(t_1+t_2+t_3)$ entering into the calculation of R_1, R_2, R_3, and R_4 (eq II-13) are different, since they correspond to different choices of j, k, l, m, and n, as shown by the Liouville-space pathways in Figure 1B. In order to calculate the trace of $\rho(t)$, we need to choose a specific representation. An adequate choice is the Wigner representation,[48,50] which for a single coordinate q and its conjugate momentum p is given by

$$\rho(p,q,t) \equiv \frac{1}{\pi\hbar}\int \mathrm{d}y\,\langle q + y|\rho(t)|q - y\rangle\,\exp(-2ipy/\hbar) \qquad \text{(II-18a)}$$

and

$$\mathrm{Tr}\,\rho(t) = \int\int \mathrm{d}p\,\mathrm{d}q\,\rho(p,q;t) \qquad \text{(II-18b)}$$

(47) Mukamel, S. *J. Phys. Chem.* **1984**, *88*, 3185. Grad, J.; Yan, Y. J.; Haque, A.; Mukamel, S. *J. Chem. Phys.* **1987**, *86*, 3441.
(48) Yan, Y. J.; Mukamel, S. *J. Chem. Phys.* **1988**, *88*, 5735; *Ibid.*, in press.
(49) Abe, S.; Mukamel, S. *J. Chem. Phys.* **1983**, *79*, 5457. Mukamel, S.; Abe, S.; Yan, Y. J.; Islampour, R. *J. Phys. Chem.* **1985**, *89*, 201.
(50) Wigner, E. *Phys. Rev.* **1932**, *40*, 749. Hillery, M.; O'Connell, R. F.; Scully, M. O.; Wigner, E. P. *Phys. Rep.* **1984**, *106*, 121.

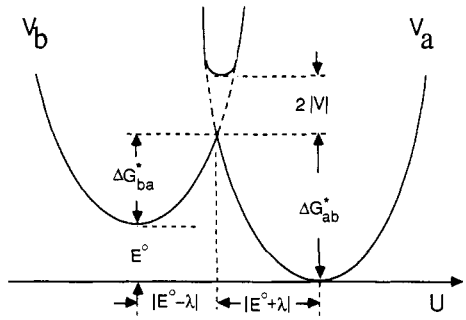

Figure 2. The potential surface for electron transfer as a function of the solvation coordinate U (eq III-10). V is the electronic coupling matrix element. λ is the solvent reorganization energy, and $E°$ is the endothermicity. ΔG_{ab}^* is the activation energy for the forward ($|a\rangle$ to $|b\rangle$) reaction, and ΔG_{ba}^* is the activation energy for the reverse reaction.

We now turn to the calculation of a rate process (isomerization, electron transfer, etc.)[46] In this case, the Hamiltonian is given by eq II-1 and II-2 with

$$H_{int} = V(|a\rangle\langle b| + |b\rangle\langle a|) \qquad \text{(II-19)}$$

Here V is the nonadiabatic coupling between the two reacting species (Figure 2). Let us denote the probability of the system to be in the $|a\rangle$ and $|b\rangle$ states by $P_a(t)$ and $P_b(t)$, respectively, where $P_a(t) + P_b(t) = 1$. In general, P_a and P_b satisfy the generalized master equation

$$dP_a/dt = -\int_0^t d\tau\, \hat{K}(t-\tau)\, P_a(\tau) + \int_0^t d\tau\, \hat{K}'(t-\tau)\, P_b(\tau) \qquad \text{(II-20)}$$

Here $\hat{K}(t-\tau)$ and $\hat{K}'(t-\tau)$ are the generalized rates for the forward and for the backward reactions, respectively. Equation II-20 can be rigorously derived from the Liouville equation (II-10a). A formally exact expression for the generalized rates may be derived by using projection operators.[46,51] It will prove convenient to introduce the Laplace transform of the generalized rate

$$K(s) = \int_0^\infty dt\, \exp(-st)\, \hat{K}(t) \qquad \text{(II-21)}$$

and similarly for $\hat{K}'(t)$. The characteristic time scale for the time variation of $\hat{K}(t-\tau)$ is related to intramolecular and solvation relaxation times. Equation II-20 is simplified considerably, when a separation of time scales exists and $\hat{K}(t-\tau)$ changes on a much faster time scale than P_a. Under these conditions, the generalized rate equation reduces to an ordinary rate equation

$$dP_a/dt = -KP_a + K'P_b \qquad \text{(II-22)}$$

where $K \equiv K(s=0)$ and $K' \equiv K'(s=0)$. The rate can, in general, be expanded in a Taylor series in the nonadiabatic coupling V. Only even powers of V contribute, i.e.[46]

$$K(s) = V^2C_2(s) - V^4C_4(s) + \ldots \qquad \text{(II-23)}$$

This series can be resummed approximately by constructing a Pade approximant. We then have

$$K(s) = \frac{V^2C_2(s)}{1 + V^2C_2(s)\,\bar{\tau}(s)} \qquad \text{(II-24)}$$

where

$$\bar{\tau}(s) \equiv C_4(s)/[C_2(s)]^2 \qquad \text{(II-25)}$$

Equation II-24 reproduces the expansion (eq II-23) to order V^4 and provides a partial resummation for the higher terms. $C_2(s)$ and $C_4(s)$ are given by

$$C_2(s) = 2\,\mathrm{Re}\int_0^\infty dt\, \exp(-st)\, J(t) \qquad \text{(II-26a)}$$

$$C_4(s) = 2\,\mathrm{Re}\int_0^\infty dt_1 \int_0^\infty dt_2 \int_0^\infty dt_3\, \exp[-s(t_1+t_2+t_3)] \times [R(t_3,t_2,t_1) - R(t_3,\infty,t_1)] \qquad \text{(II-26b)}$$

$C_2(s)$ is related to the linear response function (eq II-11), whereas $C_4(s)$ is related to the nonlinear response function (eq II-12). The nature of the rate process is determined by the adiabaticity parameter

$$\nu \equiv V^2C_2(s)\,\bar{\tau}(s) \qquad \text{(II-27)}$$

For $\nu \ll 1$, the rate process is nonadiabatic, and the rate is given by

$$K_{NA}(s) = V^2C_2(s) \qquad \text{(II-28a)}$$

In the other extreme $\nu \gg 1$, the rate process becomes adiabatic, and

$$K_{AD}(s) = 1/\bar{\tau}(s) \qquad \text{(II-28b)}$$

$\bar{\tau}(s)$ is the characteristic solvent time scale which controls the adiabaticity of the rate process. The precise definition of $\bar{\tau}(s)$ (eq II-25) is an important result of the present formulation. This will be more clearly demonstrated in the coming sections, where we shall evaluate $\bar{\tau}(s)$ for some specific models of the system–solvent interaction. As the solvent time scale becomes longer, ν increases, and a nonadiabatic rate will eventually turn adiabatic with a rate equal to the proper inverse solvent time scale. A similar expression can be derived for the reverse rate $K'(s)$ by interchanging all a and b indexes. An alternative form for the rate which has a different dependence on the nonadiabatic coupling was postulated in the literature.[16] That form is based on the Landau–Zener expression, and like eq II-24 it interpolates between the nonadiabatic limit whereby the rate is proportional to V^2 and the adiabatic limit where it is independent of V. We have considered that form as well (eq 7.6 in ref 46a). Our derivation shows, however, that eq II-24 provides an exact summation of the perturbative series for K in the static limit discussed below and should be preferred over the Landau–Zener form. We have thus established a fundamental connection between four-wave-mixing spectroscopy and molecular rate processes. We have shown how the nonlinear optical properties and the rate processes can both be expressed in terms of correlation functions of the system, which are formally identical. In the next section, we shall develop explicit expressions for these correlation functions.

III. Coupling to a Damped Harmonic Coordinate

In the previous section, we derived formal expressions for the optical susceptibilities $\chi^{(1)}$ and $\chi^{(3)}$ and for molecular rate processes in terms of the same response functions $J(t)$ and $R(t_3,t_2,t_1)$. We shall now develop a specific model for the system–solvent interaction and derive explicit expressions for these response functions. The model assumes a single harmonic coordinate, coupled to the electronic system and to a bath. The Hamiltonians H_a and H_b are given by

$$H_a = \tfrac{1}{2}\hbar\omega(p^2 + q^2) + H_B \qquad \text{(III-1a)}$$

$$H_b = \tfrac{1}{2}\hbar\omega[p^2 + (q + D)^2] + E° + H_B \qquad \text{(III-1b)}$$

Here p and q are the dimensionless momentum and coordinate, and D is a dimensionless displacement of the equilibrium position between the two states. H_B is a bath Hamiltonian. In spectroscopy, this model represents a molecule with a single vibrational mode which is strongly optically active,[43] and $E° \equiv \hbar\omega_{ba}$ is the fundamental 0–0 transition energy. In isomerization, the mode q is the isomerization coordinate which is treated here by using a nonadiabatic picture, and $E°$ is the standard free energy of the forward $|a\rangle$ to $|b\rangle$ isomerization. Solvation effects arising from the solvent fast electronic degrees of freedom are included in $E°$. The same model applies also to electron transfer, whereby q is a macroscopic solvation coordinate.[46] This will be discussed in the next section. The effect of the bath (H_B) will be treated here approximately by assuming that the oscillator satisfies a generalized Langevin equation.[45,51] The effect of H_B is then included

(51) Zwanzig, R. *Physica (Amsterdam)* **1964**, *30*, 1109.
(52) Loring, R. F.; Mukamel, S. *J. Chem. Phys.* **1987**, *87*, 1272.

in the random force and the friction of the Langevin equation (see eq III-5). We need to calculate the LGF $\rho(t)$ (eq II-15), whose time evolution is given by

$$\rho(t+t_0) = G_{jk}(t)\,\rho(t_0) = \exp(-iH_j t)\,\rho(t_0)\exp(iH_k t) \qquad \text{(III-2)}$$

jk being either aa, bb, ab, or ba, depending on the specific term being calculated and on the time interval (t_1, t_2, or t_3). We shall assume that in the Wigner picture $\rho(p,q,t)$ is given at all times by[48]

$$\rho(p,q,t) = \frac{\sigma_0}{\pi(2\bar{n}+1)}\exp\left\{-\frac{(q-\sigma_1)^2+(p-\sigma_2)^2}{2\bar{n}+1}\right\} \qquad \text{(III-3a)}$$

Here

$$\bar{n} = [\exp(\hbar\omega/kT) - 1]^{-1} \qquad \text{(III-3b)}$$

is the thermally averaged occupation number of the oscillator. $\rho(p,q,t)$ is characterized by three time-dependent parameters, $\sigma_0(t)$, $\sigma_1(t)$, and $\sigma_2(t)$, defined as follows

$$\sigma_0(t) = \mathrm{Tr}\,[\rho(t)] \qquad \text{(III-4a)}$$

$$\sigma_1(t) = \mathrm{Tr}\,[q\rho(t)] \qquad \text{(III-4b)}$$

$$\sigma_2(t) = \mathrm{Tr}\,[p\rho(t)] \qquad \text{(III-4c)}$$

We have shown that $\sigma_0(t)$, $\sigma_1(t)$, and $\sigma_2(t)$ satisfy the following equations of motion:[48]

$$\dot{\sigma}_0(t) = i\xi D\omega[\sigma_1(t) + D/2]\sigma_0(t) \qquad \text{(III-5a)}$$

$$\dot{\sigma}_1(t) = \omega\sigma_2(t) + i\xi(\bar{n}+1)D\omega \qquad \text{(III-5b)}$$

$$\dot{\sigma}_2(t) = -\omega[\sigma_1(t) + \tfrac{1}{2}D'] - \int_0^t d\tau\,\hat{\gamma}(t-\tau)\,\sigma_2(\tau) \qquad \text{(III-5c)}$$

Here $\hat{\gamma}(t-\tau)$ represents a time-dependent friction kernel resulting from the coupling with the solvent. The parameters ξ and D' depend on which propagation $G_{jk}(t)$ we consider: for jk = aa we have $\xi = 0$, $D' = 0$; for jk = bb we have $\xi = 0$, $D' = 2D$; for jk = ab we have $\xi = 1$, $D' = D$; and for jk = ba we have $\xi = -1$ and $D' = D$. We have solved eq III-5 and obtained $\rho(t)$ and $\rho(t_1+t_2+t_3)$. By taking the trace (eq II-16 and II-17), we then obtained the following expressions for $J(t_1)$ and $R_\alpha(t_3,t_2,t_1)$ (α = 1, ..., 4):

$$J(t_1) = \exp[-iE^\circ t_1]\exp[-g(t_1)] \qquad \text{(III-6)}$$

$$R_1(t_3,t_2,t_1) = \exp[-iE^\circ(t_3+t_1)]\exp[-g^*(t_3) - g(t_1)]\exp[-f_+(t_3,t_2,t_1)] \qquad \text{(III-7a)}$$

$$R_2(t_3,t_2,t_1) = \exp[-iE^\circ(t_3-t_1)]\exp[-g^*(t_3) - g^*(t_1)]\exp[f_+^*(t_3,t_2,t_1)] \qquad \text{(III-7b)}$$

$$R_3(t_3,t_2,t_1) = \exp[-iE^\circ(t_3-t_1)]\exp[-g(t_3) - g^*(t_1)]\exp[f_-^*(t_3,t_2,t_1)] \qquad \text{(III-7c)}$$

$$R_4(t_3,t_2,t_1) = \exp[-iE^\circ(t_3+t_1)]\exp[-g(t_3) - g(t_1)]\exp[-f_-(t_3,t_2,t_1)] \qquad \text{(III-7d)}$$

where

$$f_\pm(t_3,t_2,t_1) = \left[\omega\int_0^{t_3} M(\tau)\,d\tau,\ 1 - M(t_3)\right]\times \begin{bmatrix} M(t_2) & -\omega^{-1}\dot{M}(t_2) \\ \omega^{-1}\dot{M}(t_2) & -\omega^{-2}\ddot{M}(t_2)\end{bmatrix}\begin{bmatrix}\omega^{-1}(\dot{g}(t_1) \pm \dot{g}(0)) \\ \omega^{-2}(\ddot{g}(t_1) - \ddot{g}(0))\end{bmatrix} \qquad \text{(III-8)}$$

Here E° is the endothermicity for the forward reaction from $|a\rangle$ to $|b\rangle$, and $g(t)$ is the line-shape function given by

$$g(t) = i\lambda\int_0^t d\tau\,M(\tau) + \Delta^2\int_0^t d\tau_1\int_0^{\tau_1} d\tau_2\,M(\tau_2) \qquad \text{(III-9)}$$

we have defined here

$$U \equiv H_b - H_a - E^\circ = \tfrac{1}{2}\hbar\omega(2Dq + D^2) \qquad \text{(III-10)}$$

$$\lambda \equiv \langle U\rho_a\rangle = \hbar\omega D^2/2 \qquad \text{(III-11)}$$

$$\Delta^2 \equiv \langle U^2\rho_a\rangle - \langle U\rho_a\rangle^2 = \hbar^2\omega^2D^2(\bar{n}+\tfrac{1}{2}) \qquad \text{(III-12)}$$

$$M(t) = L^{-1}\left\{\frac{s+\gamma(s)}{s^2 + s\gamma(s) + \omega^2}\right\} \qquad \text{(III-13)}$$

and

$$\gamma(s) = \int_0^\infty dt\,\exp(-st)\,\hat{\gamma}(t) \qquad \text{(III-14)}$$

L^{-1} in eq III-13 represents the inverse Laplace transform. Another equivalent expression for $M(t)$ is given by eq IV-4, in terms of a correlation function of U. We have $M(0) = 1$ and $M(\infty) = 0$. We further have (cf. eq III-8)

$$f_\pm(t_3,\infty,t_1) = 0 \qquad \text{(III-15)}$$

$R_\alpha(t_3,\infty,t_1)$ may thus be obtained from eq III-7 by setting the $\exp(f_+)$ and the $\exp(f_-)$ factors equal to 1. Equations III-6–III-15 allow us to calculate $C_2(s)$ and $C_4(s)$ and the generalized rate $K(s)$ (eq II-24). We shall consider now a limiting case, in which the final expression for the rate is greatly simplified. To that end, let us examine eq II-13 more closely. During the time intervals t_1 and t_3, the system is in an off-diagonal element of the density matrix (a "coherence") ab or ba. During the t_2 interval, however, the system is in a diagonal element (a "population") aa or bb. The time evolution of the coherences is dominated by fast dephasing processes, which make their characteristic time scale much shorter than that of the populations. In the terminology of spectral line shapes, these correspond to pure dephasing processes,[40] which are usually the major contribution to spectral line widths in condensed phases. We, therefore, assume that t_1, $t_3 \ll t_2$ and expand ln $R_\alpha(t_3,t_2,t_1)$ in a Taylor series in t_1 and t_3, retaining only the lowest order contributions to the real part and to the imaginary part, resulting in the *static limit* for the response functions:

$$R_1(t_3,t_2,t_1) = \exp[-i(E^\circ+\lambda)(t_1+t_3)]\exp\{-(\Delta^2/2)[t_1^2 + t_3^2 + 2M(t_2)t_1t_3]\} \qquad \text{(III-16a)}$$

$$R_3(t_3,t_2,t_1) = \exp[-i(E^\circ+\lambda)t_1 - i(E^\circ-\lambda)t_3]\exp\{-(\Delta^2/2)\times [t_1^2 + t_3^2 + 2M(t_2)t_1t_3] - i2\lambda M(t_2)t_3\} \qquad \text{(III-16b)}$$

$$R_2(t_3,t_2,t_1) = R_1^*(-t_3,t_2,t_1) \qquad \text{(III-16c)}$$

and

$$R_4(t_3,t_2,t_1) = R_3^*(-t_3,t_2,t_1) \qquad \text{(III-16d)}$$

We further make the same short-time expansion for $J(t_1)$, appearing in $C_2(s)$ in the *denominator* of eq II-24 (but not the numerator). Assuming that ordinary rate equations hold (eq II-22), we shall calculate the rate by substituting eq II-16 in eq II-24 and II-26 and setting $s = 0$, resulting in[46]

$$K = \frac{2\pi(V^2/\hbar)\sigma(E^\circ)}{1 + (2\pi)^{1/2}[V^2/(\Delta\hbar)]\left[\tau\left(\frac{E^\circ-\lambda}{\Delta}\right) + \tau\left(\frac{E^\circ+\lambda}{\Delta}\right)\right]} \qquad \text{(III-17)}$$

where $\sigma(E^\circ)$ is the absorption line-shape function

$$\sigma(E^\circ) = (2\pi)^{-1}\int_{-\infty}^{\infty} dt\,\exp(-iE^\circ t)\exp[-g(t)] \qquad \text{(III-18)}$$

$\tau(z)$ is the solvent time scale function, given by

$$\tau(z) = \exp\left(-\frac{z^2}{2}\right)\int_0^\infty dt\left\{\frac{1}{[1-M^2(t)]^{1/2}}\exp\left[\frac{z^2M(t)}{1+M(t)}\right] - 1\right\} \qquad \text{(III-19)}$$

If we further invoke the short-time approximation for $g(t)$ in eq III-18, we have

$$\sigma(E^\circ) = \frac{1}{(2\pi)^{1/2}\Delta} \exp\left[-\frac{(E^\circ + \lambda)^2}{2\Delta^2}\right] \quad \text{(III-20a)}$$

This is the *static limit* of the theory of spectral line shapes.[40,53] In the high-temperature limit ($kT \gg \hbar\omega$), eq III-12 assumes the form

$$\Delta^2 = \hbar\omega D^2 kT = 2\lambda kT \quad \text{(III-20b)}$$

Upon the substitution of eq III-20 in eq III-17, the rate assumes the activated form

$$K = A \exp(-\Delta G_{ab}^*/kT) \quad \text{(III-21a)}$$

where the activation free energy is

$$\Delta G_{ab}^* = \frac{(E^\circ + \lambda)^2}{4\lambda} \quad \text{(III-21b)}$$

and the preexponential factor is

$$A = \frac{(2\pi)^{1/2}(V^2/\Delta\hbar)}{1 + (2\pi)^{1/2}(V^2/\Delta\hbar)\left[\tau\left(\frac{E^\circ - \lambda}{\Delta}\right) + \tau\left(\frac{E^\circ + \lambda}{\Delta}\right)\right]} \quad \text{(III-21c)}$$

In this case, the reverse rate K' is related to K by the simple detailed balance condition

$$K'/K = \exp(-E^\circ/kT) \quad \text{(III-22)}$$

Using eq III-17 or eq III-21c, we note that the adiabaticity parameter is now given by

$$\nu = (2\pi)^{1/2}(V^2/\Delta\hbar)\left[\tau\left(\frac{E^\circ - \lambda}{\Delta}\right) + \tau\left(\frac{E^\circ + \lambda}{\Delta}\right)\right] \quad \text{(III-23)}$$

When $\nu \ll 1$, the rate process is nonadiabatic

$$K_{NA} = 2\pi(V^2/\hbar)\sigma(E) \qquad \nu \ll 1 \quad \text{(III-24a)}$$

whereas when $\nu \gg 1$, it is adiabatic

$$K_{AD} = (2\pi)^{1/2}\Delta\sigma(E^\circ)/\left[\tau\left(\frac{E^\circ - \lambda}{\Delta}\right) + \tau\left(\frac{E^\circ + \lambda}{\Delta}\right)\right] \qquad \nu \gg 1 \quad \text{(III-24b)}$$

Equations III-17–III-21 constitute a closed expression for the rate of molecular processes. The precise conditions which $M(t)$ should satisfy for this expression to hold are given in ref 46. E°, V, Δ, and λ are *static* quantities. E° is the endothermicity and V is the nonadiabatic coupling whereas Δ and λ are related to the coupling strength between the molecule and the solvent. $M(t)$ on the other hand is a *dynamical* quantity which depends on the solvent dynamics and friction. The precise definition of the solvent time scale function $\tau(z)$ (eq III-19) is one of the major results of the present formulation. $\tau[(E^\circ - \lambda)/\Delta]$ results from R_1 and R_2 (eq III-16) and represents a characteristic solvent relaxation time scale when the system is in the state $|b\rangle$. $\tau[(E^\circ + \lambda)/\Delta]$ results from R_3 and R_4 and represents a solvent relaxation time scale when the system is in the state $|a\rangle$.[46] A further discussion of the microscopic dynamics underlying $\tau(z)$ will be given in section VII. For the sake of clarity in the presentation, we have considered, in this section, a single coordinate q. One of the advantages of the present approach is that the incorporation of additional coordinates (e.g., more intramolecular vibrations) is straightforward. Equation III-3a should then be replaced by a multivariate Gaussian distribution, which can be calculated by equations similar to eq III-5. Furthermore, in the present model, we assumed that the harmonic coordinate has the same frequency in H_a and H_b. When allowing for different frequencies, we need to generalize the Gaussian equation (III-3a) by allowing the second moments of p and q to vary with time as well. These extensions are presented elsewhere.[48]

(53) Bloembergen, N.; Purcell, E. M.; Pound, R. V. *Phys. Rev.* **1948**, *73*, 679. Anderson, P. W.; Weiss, P. R. *Rev. Mod. Phys.* **1953**, *25*, 269. Kubo, R. *Adv. Chem. Phys.* **1969**, *15*, 101.

IV. Electron-Transfer Rates in Polar Solvents

The model considered in the previous section and the expressions for the rate apply to electron transfer (ET) in a polar solvent as well. The basic model for ET consists of the charge-transfer system which has two states corresponding to the electron on the donor or the acceptor site and denoted $|a\rangle$ and $|b\rangle$, respectively. The system is interacting electrostatically with a polar solvent. The electric field at position $\mathbf{r}$, created by the system in states $|a\rangle$ and $|b\rangle$, is denoted $\mathbf{D}_a(\mathbf{r})$ and $\mathbf{D}_b(\mathbf{r})$, respectively. The endothermicity of the reaction is denoted by E°. It includes the interaction energy with the solvent electronic degrees of freedom, which are assumed to respond instantaneously to the charge rearrangements in the system. The states $|a\rangle$ and $|b\rangle$ are coupled by a nonadiabatic electronic matrix element V (eq II-19). The Hamiltonian of the system is given by eq II-1 and II-2 with

$$H_m = H_B - \int d\mathbf{r}\, P(\mathbf{r})\, D_m(\mathbf{r}) \qquad m = a, b \quad \text{(IV-1)}$$

Here H_B is the pure solvent Hamiltonian. $P(\mathbf{r})$ is the solvent polarization, and its interaction with the molecule is given by the second term in eq IV-1.

We now introduce the solvation coordinate

$$U \equiv H_b - H_a = -\int d\mathbf{r}\, [D_b(\mathbf{r}) - D_a(\mathbf{r})]P(\mathbf{r}) \quad \text{(IV-2)}$$

The statistical properties of U may be related to the frequency-dependent dielectric function of the solvent[54,55]

$$\epsilon(\omega) = \epsilon_\infty + (\epsilon_0 - \epsilon_\infty)F(\omega) \quad \text{(IV-3)}$$

Here ϵ_0 is the static ($\omega = 0$) and ϵ_∞ is the high-frequency (optical) value of $\epsilon(\omega)$, and the frequency dependence of $F(\omega)$ reflects the dynamical dielectric relaxation of the solvent. We have shown[46] that the rate in the static limit is given by eq III-17–III-19 or eq III-21 with

$$M(t) = \frac{[\langle U(t)U\rho_a\rangle + \langle UU(t)\rho_a\rangle]/2 - \langle U\rho_a\rangle^2}{\Delta^2} \quad \text{(IV-4)}$$

where

$$U(t) \equiv \exp(iH_a t)U\exp(-iH_a t) \quad \text{(IV-5)}$$

Expanding the rate perturbatively around H_B, we get in the high-temperature limit[46]

$$\lambda \equiv \langle U\rho_a\rangle = \frac{1}{8\pi}\int d\mathbf{r}\, [D_a(\mathbf{r}) - D_b(\mathbf{r})]^2[1/\epsilon_\infty - 1/\epsilon_0] \quad \text{(IV-6)}$$

$$\Delta^2 \equiv \langle U^2\rho_a\rangle - \langle U\rho_a\rangle^2 = 2\lambda kT \quad \text{(IV-7)}$$

and

$$M(t) = Q(t)/Q(0) \quad \text{(IV-8a)}$$

with

$$Q(t) = \frac{1}{2\pi i}\int_{-\infty}^{\infty}\frac{d\omega}{\omega}\exp(i\omega t)\left[\frac{1}{\epsilon(\omega)} - \frac{1}{\epsilon_0}\right] \quad \text{(IV-8b)}$$

and $Q(0)$ is equal to the *Pekar factor*:

$$Q(0) = 1/\epsilon_\infty - 1/\epsilon_0 \quad \text{(IV-8c)}$$

Equations III-17–III-19, or eq III-21, together with eq IV-6–IV-8 provide a closed expression for the ET rate and relate it to properties of the ET system and to the solvent dielectric function. Let us briefly comment on the significance of these quantities. The *solvent dynamics* are contained in $M(t)$, which is the normalized correlation function of the solvation coordinate. $M(t)$ enters eq III-17 via the line-shape function $\sigma(E^\circ)$ and through the function $\tau(z)$ (eq III-19), which is a characteristic relaxation

(54) (a) Debye, P. *Polar Molecules*; Dover: New York, 1929. (b) Fröhlich, H. *Theory of Dielectrics*; Oxford: London, 1949.
(55) Böttcher, C. J. F.; Bordewijk, P. *Theory of Electric Polarization*; Elsevier: Amsterdam, 1978; Vol. II.

time for solvent fluctuations, when the reaction coordinate is perturbed around the value $E^\circ \pm \lambda$. $\tau(z)$ thus represents the solvent time scale relevant for the ET rate. In the static limit, which often holds in ET reactions, $\sigma(E^\circ)$ becomes independent of the solvent time scale (see eq III-20), and the only dependence on solvent dynamics is then contained in $\tau(z)$. The other quantities appearing in eq III-17 (Δ and λ) depend on the Pekar factor which is related to the *solvent polarity* but not to its dynamics. λ is the reorganization energy of the solvent[5] and measures the coupling strength of the charge-transfer system to the nuclear degrees of freedom of the solvent. One of the important conclusions from eq III-21b, together with eq IV-6, is that the activation free energy depends on the solvent only through the Pekar factor. The solvent dynamics do not affect ΔG_{ab}^*. Marcus[5] has derived this relation for Debye solvents (eq V-6). The present theory shows that this result is valid for arbitrary non-Debye solvents as well. It should further be noted that, in general, a polar solvent is characterized by a frequency- and wavevector-dependent dielectric function $\epsilon(\mathbf{k},\omega)$. In the present analysis, we used only the long-wavelength ($\mathbf{k} = 0$) limit of $\epsilon(\mathbf{k},\omega)$. It is possible, however, without a major difficulty to incorporate spatial dispersion and the full $\epsilon(\mathbf{k},\omega)$ into the present theory.[46,52]

V. The Debye–Smoluchowski–Kubo Model

In the previous section, we developed a closed expression for rate processes in the static limit, which is valid for a solvation correlation function $M(t)$ with an arbitrary time dependence. In this section, we consider the special case, where $M(t)$ assumes an exponential form:

$$M(t) = \exp(-\Lambda t) \tag{V-1}$$

This form is a limiting case of various models of solvation. When eq V-1 holds, it is possible to derive exact expressions for $C_2(s)$ and $C_4(s)$ (eq II-26), resulting in an expression for the rate (eq II-24), which is not restricted to the static limit. We shall first discuss several physical models for which eq V-1 holds and then derive the corresponding expressions for $C_2(s)$ and $C_4(s)$. We shall start with the damped oscillator model introduced in section III and for simplicity assume that the friction is independent of frequency, i.e.

$$\hat{\gamma}(t) = 2\gamma\delta(t) \tag{V-2a}$$

$$\gamma(s) = \gamma(s=0) = \gamma \tag{V-2b}$$

In this case, eq III-13 results in

$$M(t) = \tfrac{1}{2}[\alpha_+ \exp(-i\alpha_-\Omega t) + \alpha_- \exp(i\alpha_+\Omega t)] \tag{V-3a}$$

with

$$\Omega = [\omega^2 - (\gamma/2)^2]^{1/2} \tag{V-3b}$$

and

$$\alpha_\pm = 1 \pm i\gamma/(2\Omega) \tag{V-3c}$$

and eq III-8 reduces to

$$f_-(t_3,t_2,t_1) = g(t_2) - g(t_2+t_3) - g(t_1+t_2) + g(t_1+t_2+t_3) \tag{V-3d}$$

$$f_+(t_3,t_2,t_1) = g^*(t_2) - g^*(t_2+t_3) - g(t_1+t_2) + g(t_1+t_2+t_3) \tag{V-3e}$$

where $g(t)$ is given by eq III-9. We shall consider now two limiting cases of eq V-3. In the absence of friction ($\gamma = 0$), we have

$$M(t) = \cos \omega t \tag{V-4a}$$

and

$$g(t) = -(D^2/2)\{(\bar{n} + 1)[\exp(-i\omega t) - 1] + \bar{n}[\exp(i\omega t) - 1]\} \tag{V-4b}$$

When $\gamma \gg \omega$, the oscillator is overdamped, and we get

$$M(t) = \exp(-\Lambda t) \tag{V-5a}$$

with

$$\Lambda = \omega^2/\gamma \tag{V-5b}$$

and

$$g(t) = \frac{i}{2}D^2\frac{\omega}{\Lambda}[1 - \exp(-\Lambda t)] + \left(\bar{n} + \frac{1}{2}\right)D^2\frac{\omega^2}{\Lambda^2}[\Lambda t - 1 + \exp(-\Lambda t)]$$

$$\approx \frac{\Delta^2}{\Lambda^2}[\Lambda t - 1 + \exp(-\Lambda t)] \tag{V-5c}$$

In the second equality of eq V-5c, we have made use of eq III-12 and neglected the imaginary part, since it is an order of ω/γ smaller than the real part. It can easily be shown that the oscillator motion in this limit is diffusive. This high-friction limit is also known as "the Smulochowski limit".[44,45] We have thus established that in the overdamped Smulochowski limit our oscillator model of section III results in the exponential correlation function (eq V-1). A stochastic model, commonly used in the theory of magnetic resonance and optical line shapes, is based on the same equation.[40,53] That model has been used to describe a variety of gases (collisional) as well as liquids and solids. Another case, where eq V-1 applies, is electron transfer in a Debye solvent. The Debye model[54,55] for the dielectric function assumes a single dielectric relaxation time τ_D

$$\epsilon(\omega) = \epsilon_\infty + (\epsilon_0 - \epsilon_\infty)\frac{1}{1 + i\omega\tau_D} \tag{V-6}$$

Upon the substitution of eq V-6 in eq IV-8 we get eq V-1 with

$$\Lambda^{-1} \equiv \tau_L = \tau_D(\epsilon_\infty/\epsilon_0) \tag{V-7}$$

Here τ_L is the *longitudinal dielectric relaxation time* of the solvent. We have thus established three physical models which result in eq V-1: the overdamped oscillator, the stochastic model of line broadening, and the Debye model of dielectric relaxation. For this model it is possible to solve $C_2(s)$ and $C_4(s)$ analytically without invoking the static limit.[43,47] We shall denote the contribution of R_1 and R_2 to $C_4(s)$ by $C_4^{(a)}(s)$ and the contribution of R_3 and R_4 to $C_4(s)$ by $C_4^{(b)}(s)$. We finally have

$$C_2(s) = 2 \text{ Re } J_0(s + iE^\circ) \tag{V-8}$$

and

$$C_4(s) = C_4^{(a)}(s) + C_4^{(b)}(s) \tag{V-9}$$

where

$$C_4^{(a)}(s) = 2 \text{ Re } \sum_{n=1}^{\infty}\frac{c^n}{n!}\frac{1}{s + n\Lambda}J_n(s + iE^\circ)[(-1)^n J_n(s + iE^\circ) + J_n^*(s + iE^\circ)] \tag{V-10a}$$

$$C_4^{(b)}(s) = 2 \text{ Re } \sum_{n=1}^{\infty}\frac{c^n}{n!}\frac{1}{s + n\Lambda}\bar{J}_n(s + iE^\circ)[(-1)^n J_n^* \times (s - iE^\circ) + J_n(s - iE^\circ)] \tag{V-10b}$$

with

$$J_n(s) \equiv \int_0^\infty dt \exp(-st) \exp[-g(t)][1 - \exp(-\Lambda t)]^n \tag{V-11a}$$

$$\bar{J}_n(s) = \int_0^\infty dt \exp(-st) \exp[-g(t)][c^*/c - \exp(-\Lambda t)]^n$$

$$= J_n(s) + \sum_{k=1}^{n}\binom{n}{k}(c^*/c - 1)^k J_{n-k}(s) \tag{V-11b}$$

and

$$g(t) = i(\lambda/\Lambda)[1 - \exp(-\Lambda t)] + (\Delta/\Lambda)^2[\Lambda t - 1 + \exp(-\Lambda t)] \tag{V-12}$$

Alternatively, we can write

$$J_n(s) = \frac{n!\Gamma(b)}{\Lambda\Gamma(b + n + 1)}M(n+1,b+n+1,c) = \frac{1}{s + \Delta^2/\Lambda}\sum_{m=0}^{\infty}\frac{(n + m)!c^m}{m!(b + 1)_{n+m}} \tag{V-13a}$$

where $M(n+1,b+n+1,c)$ is the confluent hypergeometric function,[43,56] and where

$$(a)_0 = 1, \quad (a)_1 = a, \ldots, \quad (a)_n = a(a+1)\ldots(a+n-1) \tag{V-13b}$$

$$b = (\Delta/\Lambda)^2 + s/\Lambda \tag{V-13c}$$

and

$$c = (\Delta/\Lambda)^2 - i\lambda/\Lambda \tag{V-13d}$$

Alternative expressions for J_n (and $\bar{J}_n$) may be derived via continued fractions or recursive relations.[43] When eq V-8–V-13 are substituted in eq II-24, we obtain an expression for the rate that is not limited to the static limit and holds when $M(t)$ is given by eq V-1.

VI. Numerical Calculations of Rate Processes, Fluorescence, and Hole-Burning Line Shapes

In this section, we present some numerical calculations for the rate and analyze its dependence on the solvation dynamics. We start with the nonadiabatic limit, where the rate is given by eq III-24a. $\sigma(E°)$ is an ordinary line-shape function. We have plotted $\sigma(E°)$ vs $E°$, which illustrates the dependence of the nonadiabatic rate on endothermicity. $M(t)$ was calculated for polar solvents via eq IV-8. The following models were used for $\epsilon(\omega)$.[46,55] The Debye model contains a single relaxation time (eq V-6). $\epsilon(\omega)$ for linear alcohols (propanol to decanol) contains three relaxation times and is given by[57]

$$\epsilon(\omega) = \epsilon_\infty + (\epsilon_0 - \epsilon_\infty)\sum_{j=1}^{3}\frac{c_j}{1 + i\omega\tau_j} \tag{VI-1a}$$

This corresponds to

$$M(t) = \sum_{j=1}^{3} c_j' \exp(-t/\tau_j') \tag{VI-1b}$$

where c_j' and τ_j' are related to c_j, τ_j, ϵ_0, and ϵ_∞ via eq IV-8. Finally, the Cole–Davidson model has a continuous distribution of Debye times

$$\epsilon(\omega) = \epsilon_\infty + \frac{\epsilon_0 - \epsilon_\infty}{(1 + i\omega\tau_0)^\beta} \tag{VI-2}$$

For all three models, we first calculated $M(t)$, using eq IV-8; we thus obtained $g(t)$ (eq III-9) and finally the line shape (eq III-18).

Let us analyze first $\sigma(E°)$ for the Debye model. $\sigma(E°)$ has a maximum at $E° + \lambda = 0$. Near the line center for $|E° + \lambda| \ll \hbar/\tau_L$ the line shape assumes a Lorentzian form:

$$\sigma(E°) = \frac{\Gamma/\pi}{(E° + \lambda)^2 + \Gamma^2} \tag{VI-3}$$

with $\Gamma = \Delta^2\tau_L/\hbar$. In the wings $|E° + \lambda| \gg \hbar/\tau_L$ the line shape is Gaussian

$$\sigma(E°) = \frac{1}{(2\pi)^{1/2}\Delta}\exp\left[-\frac{(E° + \lambda)^2}{2\Delta^2}\right] \tag{VI-4}$$

The full width at half-maximum of the line shape is given by[43]

$$\Gamma_0 = \frac{2.355 + 1.76\,\kappa}{1 + 0.85\kappa + 0.88\kappa^2}\Delta \tag{VI-5}$$

The line shape $\sigma(E°)$ is dominated by the parameter

$$\kappa = \frac{\hbar}{\Delta\tau_L} = \frac{\hbar}{(2\lambda kT)^{1/2}\tau_L} \tag{VI-6}$$

The following conclusions may be obtained by a close examination of eq VI-3–VI-6. For $\kappa \gg 1$ the line shape is Lorentzian over many widths since $\Gamma_0 \ll \hbar/\tau_L$. For $\kappa \ll 1$ the line is Gaussian since $\Gamma_0 \gg \hbar/\tau_L$, and the onset of Gaussian behavior occurs near the line center. In Figure 3 we show $\sigma(E°)$ for various values of τ_L (as indicated). The transition from Lorentzian to Gaussian as τ_L increases is clearly demonstrated. In Figure 4, we display $\sigma(E°)$ for linear alcohols (eq VI-1), and in Figure 5 for the Cole–Davidson model (eq VI-2). In all cases, the line shape is Lorentzian in the center and Gaussian in the wings, as is the case for the Debye model. The actual line shapes are, however, distinctly different and reflect the multiple time scales of $M(t)$. In

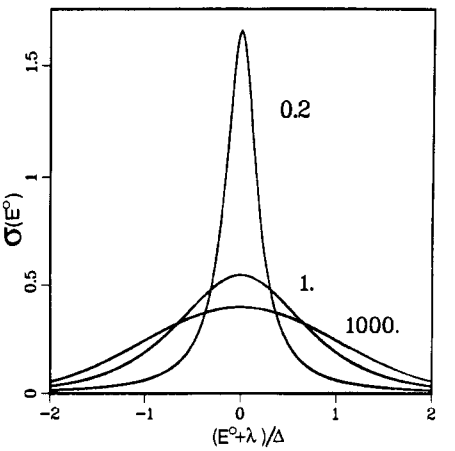

Figure 3. The line-shape function $\sigma(E°)$ for the Debye model is displayed for different values of the longitudinal dielectric relaxation time τ_L.[46] Each curve is labeled by the corresponding relaxation time τ_L, given in units of $\hbar/\Delta$. As τ_L increases, $\sigma(E°)$ changes from a Lorentzian to a Gaussian.

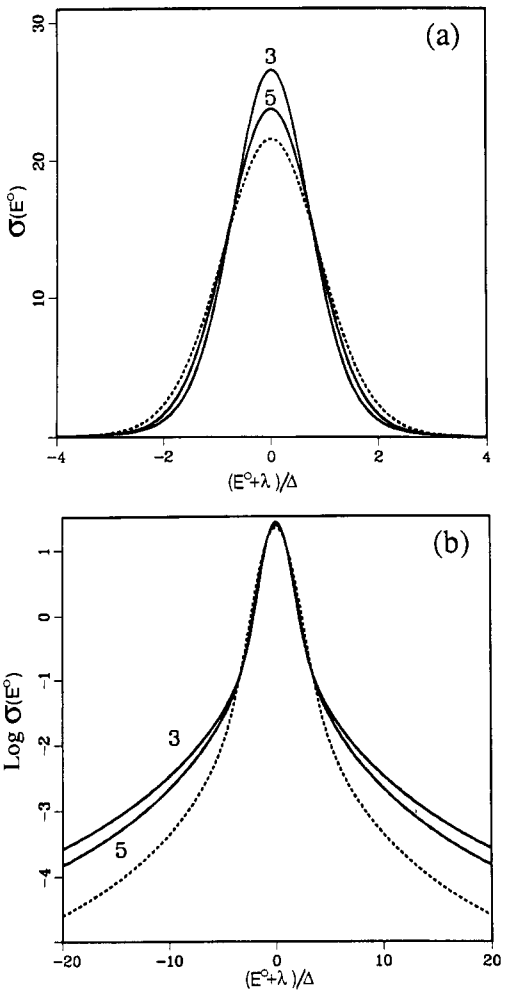

Figure 4. (a) The line shape $\sigma(E°)$ (in $(cm^{-1})^{-1}$) is plotted for propanol (3) and pentanol (5), at 20 °C with $\Delta = 0.53$ cm^{-1}. The dashed line gives $\sigma(E°)$ for a Debye model with τ_D equal to τ_1 of propanol and the ϵ_0 and ϵ_∞ of propanol.[46] (b) Same as (a), plotted on a logarithmic scale (base 10).

(56) Abramowitz, M.; Stegun, I. A. *Handbook of Mathematical Functions*; Dover: New York, 1970.
(57) Garg, S. K.; Smyth, C. P. *J. Phys. Chem.* **1965**, *69*, 1294.

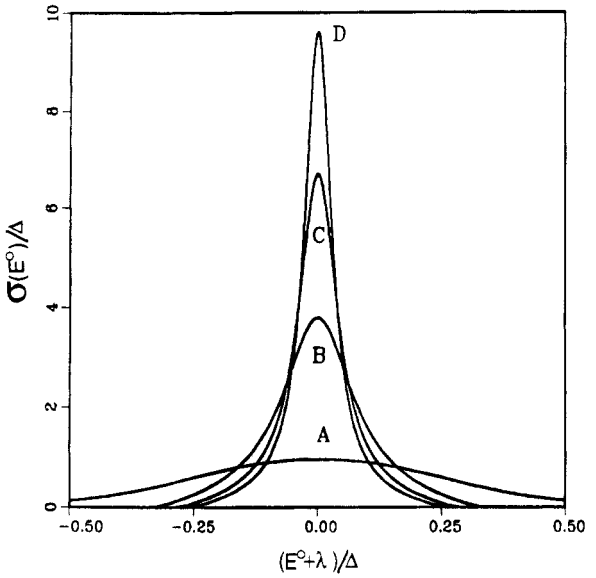

Figure 5. The function $\sigma(E^\circ)/\Delta$ is plotted for the Cole–Davidson model with $\beta = 0.5$ and $\tau_0 = \hbar/\Delta$. Curves A, B, C, and D correspond respectively to $\epsilon_\infty/\epsilon_0 = 0.82$, 0.17, 0.096, and 0.067.

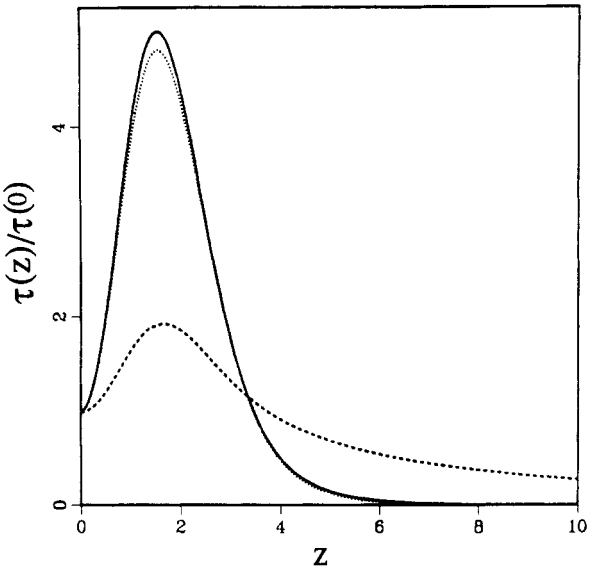

Figure 6. The solvent time scale function $\tau(z)/\tau(0)$ is plotted for a Debye solvent (dashed curve), for propanol (solid curve), and for hexanol (dotted curve) at 20 °C.[46] For linear n-alcohols with $n = 1$–10, the $\tau(z)/\tau(0)$ curve is very similar.

order to study the transition to the adiabatic regime, we shall consider now the solvent time scale function $\tau(z)$, which controls the adiabaticity parameter. In Figures 6 and 7, we display $\tau(z)$ vs z for the linear alcohols and for the Cole–Davidson model. In each figure we display also $\tau(z)$ for the Debye model. For the Debye model $\tau(0) = (\ln 2)\tau_L$ and $\tau(z)/\tau(0)$ is a single curve, independent of ϵ_0 or ϵ_∞, whereas for the other cases $\tau(z)/\tau(0)$ does depend on ϵ_0 and ϵ_∞ as well. The curves look qualitatively similar. They all have a maximum and vanish for large z. We have shown that the asymptotic behavior of $\tau(z)$ for $z \gg 1$ is $\sim z^{-1}$ for the Debye model and for the linear alcohols and is $\sim z^{1-2/\beta}$ for the Cole–Davidson model.[46] Our analysis of $\sigma(E^\circ)$ and $\tau(z)$ allows us to predict the variation of the rate (eq III-17) with the solvent time scale and the transition to the adiabatic regime. We shall perform the analysis for the Debye model. The other models are qualitatively similar.[46] We shall start with the nonadiabatic rate with very short τ_L. In this case, the line shape $\sigma(E^\circ)$ will be a narrow Lorentzian (eq VI-3) (motional narrowing), and its width is $\Gamma = \Delta^2\tau_L/\hbar \to 0$. We then expect that $|E^\circ + \lambda| \gg \Gamma$, so that $\sigma(E^\circ) \sim \Gamma$. As τ_L is increased, the Lorentzian width grows, and we get $|E^\circ + \lambda| < \Gamma$, which implies that $\sigma(E^\circ) \sim \Gamma^{-1}$. We thus

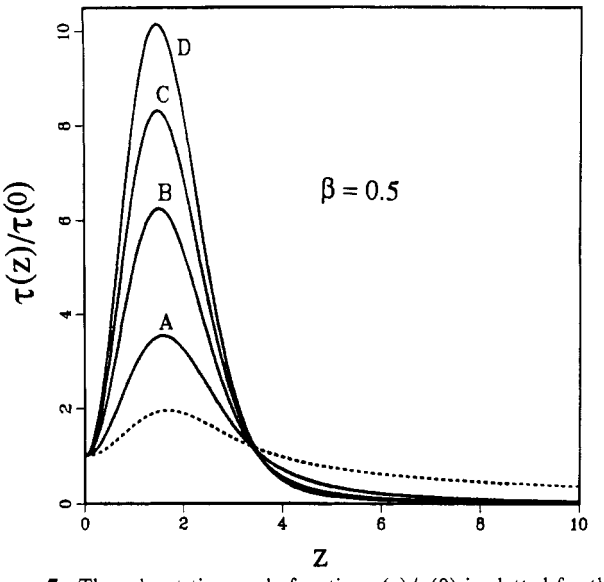

Figure 7. The solvent time scale function $\tau(z)/\tau(0)$ is plotted for the Cole–Davidson model with $\beta = 0.5$. Curves A, B, C, and D correspond respectively to $\epsilon_\infty/\epsilon_0 = 0.82$, 0.17, 0.096, and 0.067. The dashed curve is for the Debye model.[46]

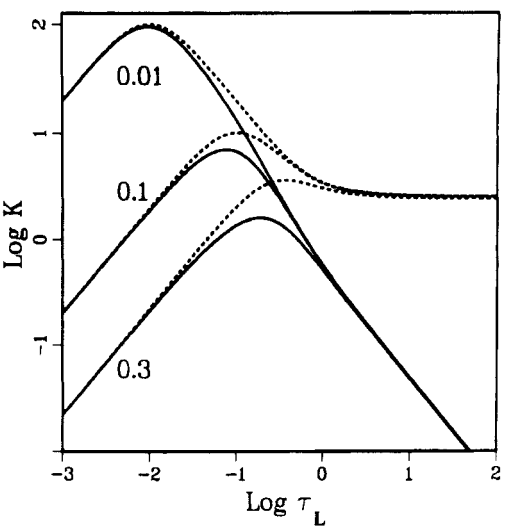

Figure 8. The ET rate versus the longitudinal relaxation time for small barriers.[46] The solid lines represent our result (eq III-17) for $\Delta = 1$, $V = 1$, and $\lambda = 0.5$. Each curve is labeled by the value of the endothermicity E°. The dashed curves are the nonadiabatic rates (eq III-24a), shown for comparison. For small τ_L the nonadiabatic limit holds, and the rate is proportional to τ_L. As τ_L increases, the nonadiabatic rate assumes a constant value independent of τ_L, whereas the complete expression (eq III-17) decreases as $1/\tau_L$. The solid lines clearly show the Kramers turnover regime. τ_L is given in units of $\hbar/\Delta$.

predict that the nonadiabatic rate will grow with τ_L when τ_L is sufficiently short, $\sigma(E^\circ) \sim \Gamma \sim \tau_L$, and will then reach a maximum and decrease with τ_L, $\sigma(E^\circ) \sim \Gamma^{-1} \sim \tau_L^{-1}$, for larger values of τ_L. When τ_L is increased even further, the line shape will eventually turn into the Gaussian (eq VI-4), and the rate will become independent of τ_L. We thus have a crossover between three regimes: the wings of a Lorentzian for very short τ_L, the center of a Lorentzian for intermediate τ_L, and the Gaussian for large τ_L. The rate when plotted vs τ_L will show a maximum and then reach a plateau. This behavior is illustrated by the dashed curves in Figure 8.

We shall now consider the transition to the adiabatic regime whereby the rate (eq III-17) gradually attains the limiting form (eq III-24b) with the solvent time scale $\tau(z)$ defined in eq III-19, together with eq V-1. The function $\tau(z)$ is proportional to τ_L (Figure 6). Since $\tau(z)$ and the adiabaticity parameter ν (eq III-23) are proportional to τ_L, we predict that, for large τ_L, the adiabatic rate will decrease as τ_L^{-1}. Using eq III-21c, we have for $\nu \gg 1$

$$A = \frac{1}{\tau\left(\frac{E^\circ - \lambda}{\Delta}\right) + \tau\left(\frac{E^\circ + \lambda}{\Delta}\right)} \sim \frac{1}{\tau_L} \qquad \text{(VI-7)}$$

The plateau regime of the nonadiabatic rate (dashed curves in Figure 8) will thus turn into a $1/\tau_L$ behavior. The solid curves in Figure 8 show the τ_L dependence of the rate (eq III-17). The variation of the rate with the solvent time scale τ_0 for the Cole–Davidson model was calculated and found to show a similar turnover behavior.[46]

The classical work of Kramers[44] provides a convenient framework for discussing solvation effects in chemical dynamics. Kramers proposed a model in which the chemical reaction dynamics is treated in terms of escape over a barrier of a particle moving in a one-dimensional potential well and subject to a stochastic Langevin force. Kramers obtained approximate solutions for the equation of motion of the particle in phase space (the Kramers equation).[44,45] His expression for the rate is the activated form (eq III-21), where the preexponential factor A is given by

$$A = \begin{cases} \eta \Delta G_{ab}^*/kT & \text{small friction} \\ \omega & \text{intermediate friction} \\ \dfrac{2\pi\omega\omega'}{\eta} & \text{large friction} \end{cases} \qquad \text{(VI-8)}$$

Kramers further derived an expression for A, which interpolates between the intermediate and the large friction regimes

$$A = (\omega/2\pi\omega')\{[\eta^2/4 + (2\pi\omega')^2]^{1/2} - \eta/2\} \qquad \text{(VI-9)}$$

Here ω is the curvature of the potential at the minimum of the reactant side, and ω' is the curvature at the point of maximum barrier height. A further depends on the solvent through the parameter

$$\eta \equiv \gamma/m \qquad \text{(VI-10)}$$

where γ is the friction coefficient of the Langevin force and m is the mass of the particle. For low friction, the solvent helps the reaction by providing energy to the molecule. The rate then grows linearly with the friction. This is the falloff regime of unimolecular kinetics.[21] At high friction, however, the energy is no longer a limiting factor, because there are strong interactions between the solvent and the molecule, and the main effect of the solvent is to slow the rate process. This arises since the motion of the particle is diffusive in this limit, and the Stokes–Einstein relation implies that the diffusion (and the reaction) rate should vary as $\sim\eta^{-1}$. This high friction limit is called "the Smoluchowski limit".[45] The nonmonotonic dependence of the rate on friction, which has a maximum at intermediate frictions, is known as the "Kramers turnover". Since τ_L is proportional to the friction γ (see eq V-5b and V-7), our rate expression (eq III-17) and Figure 8 reproduce the three regimes of Kramers and the turnover curve.

The present formulation establishes a general fundamental connection between the solvent correlation functions which affect nonlinear optical processes and the dynamics of rate processes in the same solvent. The transition to the adiabatic limit is strikingly analogous to the saturation of spectral line shapes in a strong radiation field (the Karplus–Schwinger line shape).[40,62] The nonlinear response function $R(t_3,t_2,t_1)$ is the fundamental quantity controlling all four-wave-mixing spectroscopies (e.g., coherent Raman, transient grating, photon echo, hole burning) as well as spontaneous two-photon processes (fluorescence and Raman line shapes). Any such spectroscopic measurement, whether time domain (femtosecond) or frequency domain, provides a piece of information regarding $R(t_3,t_2,t_1)$. We have recently used the expressions for R_1, R_2, R_3, and R_4 (eq III-16) for the Debye model to calculate $\chi^{(3)}$ and the time- and frequency-resolved fluorescence and hole-burning line shapes of a polar solute in polar solvents.[42] We predict a significant narrowing of both line shapes at short times, followed by a broadening, and a time-dependent Stokes shift. The theory shows how to extract solvation parameters from such measurements. The fluorescence of a model solute is shown in Figure 9, and the hole-burning line shape is shown in Figure 10. It should further be noted that the present treatment of solvation can be applied to the mobility of a charged particle (electron, ion) in a polar solvent (the polaron problem).[36,58-61] Recent ultrafast spectra of solvated electrons in various solvents provide an excellent probe for the dynamics of solvation in this system. The present derivation allows the direct use of optical measurements in predicting reaction rates. An example of such a connection is provided by the use of rotational relaxation times (obtained, e.g., from fluorescence depolarization) as a measure of the solvent friction in the Kramers equation. This relation was postulated[4,19,22] and proved useful in several systems, such as the isomerization of diphenylbutadiene and stilbene in alkanes.[22] The present formulation may allow a more direct derivation of such relationships.

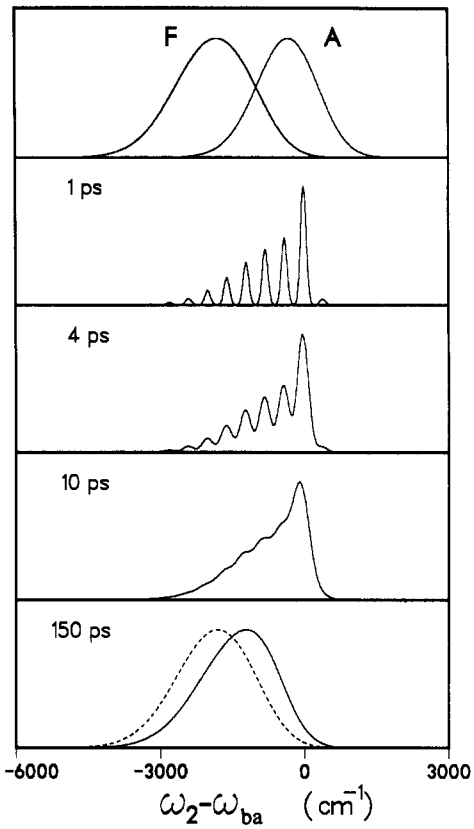

Figure 9. The top frame shows the steady-state absorption and fluorescence spectra of a model solute with one vibrational mode in ethanol at 247 K. The following frames show the fluorescence spectrum, measured at successively later times, after the application of a 1-ps excitation pulse.[42] Each spectrum is labeled with the observation time. The steady-state fluorescence spectrum is repeated with the dashed curve in the final frame. The absorption spectrum is plotted vs $\omega_{ba} - \omega_1$, and the fluorescence spectra are plotted vs $\omega_2 - \omega_{ba}$. For the fluorescence spectra, $\omega_1 = \omega_{ba}$. In the electronic ground state, the solute vibrational frequency is 400 cm^{-1}, and in the excited state, the frequency is 380 cm^{-1}. The dimensionless displacement is 1.4. The permanent dipole moment changes by 10 D upon electronic excitation. The Onsager radius is 3 Å. The longitudinal dielectric relaxation time, τ_L, is 150 ps.

VII. Discussion

The main theme of this article is the development of a basic relation between the calculation of linear and nonlinear optical line shapes and molecular rate processes. Both dynamical observables were expressed in terms of the same response functions

(58) Feynman, R. *Statistical Mechanics, a Set of Lectures*; Benjamin: Reading, MA, 1972.
(59) Kenney-Wallace, G. A.; Jonah, C. D. *J. Phys. Chem.* **1982**, *86*, 2572.
(60) *Polarons in Ionic Crystals and Polar Semiconductors*; DeVreese, J. T., Ed.; North-Holland: Amsterdam, 1972.
(61) "Proceedings of the Sixth International Conference on Excess Electrons and Metal–Ammonia Solutions, Colloque Weyl VI", *J. Phys. Chem.* **1984**, *88*, 3699.
(62) Karplus, R.; Schwinger, J. *Phys. Rev.* **1948**, *73*, 1020.

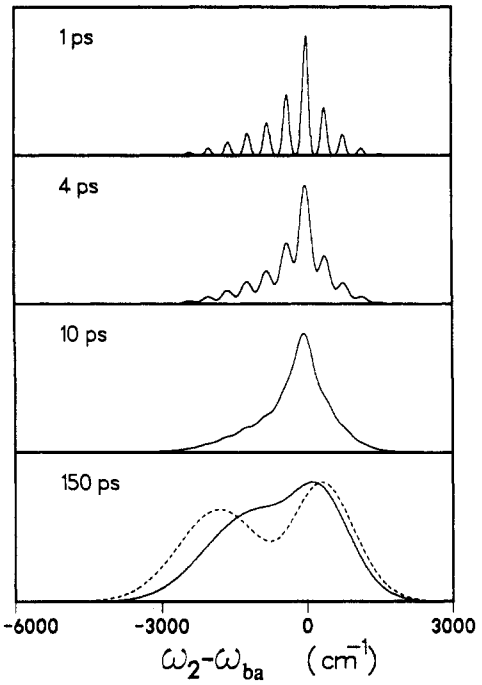

Figure 10. Hole-burning line shapes of a solute with one vibrational mode in ethanol at 247 K, following a 1-ps pump pulse.[42] Each frame is labeled with the delay time between pump and probe. The dashed curve in the final frame represents the hole-burning line shape when the delay time is much longer than τ_L. $\omega_1 = \omega_{ba}$. All parameters are the same as Figure 9.

$J(t_1)$ and $R(t_3,t_2,t_1)$. These functions may be calculated by propagating a Liouville-space generating function (LGF).[48] The LGF starts with the equilibrium density matrix of the system ρ_a. It then undergoes a propagation or a sequence of propagations, in which the Hamiltonians acting from the left and from the right are not necessarily the same, i.e.

$$\rho(t+t_0) = G_{jk}(t)\ \rho(t_0) \equiv \exp(-iH_j t)\ \rho(t_0)\ \exp(iH_k t) \qquad \text{(VII-1)}$$

which satisfies the equation

$$\dot{\rho} = -i(H_j\rho - \rho H_k) \qquad \text{(VII-2)}$$

The choice of j and k depends on the particular diagram and time interval (see Figure 1). We reiterate that the LGF is not a density matrix, and its normalization (σ_0) is not conserved. It should be viewed as a generating function for calculating correlation functions.[48,49] We found it natural to formulate the problem in Liouville space. It is formally possible to rewrite the expressions for R_1, R_2, R_3, and R_4 by using an ordinary (not Liouville space) correlation function.[38,40] We then have

$$\begin{aligned}
|\mu|^4 R_1(t_3,t_2,t_1) &= F(t_1,t_1+t_2,t_1+t_2+t_3,0)\\
|\mu|^4 R_2(t_3,t_2,t_1) &= F(0,t_1+t_2,t_1+t_2+t_3,t_1)\\
|\mu|^4 R_3(t_3,t_2,t_1) &= F(0,t_1,t_1+t_2+t_3,t_1+t_2)\\
|\mu|^4 R_4(t_3,t_2,t_1) &= F(t_1+t_2+t_3,t_1+t_2,t_1,0)
\end{aligned} \qquad \text{(VII-3)}$$

with the four-point correlation functions of the dipole operators

$$F(\tau_1,\tau_2,\tau_3,\tau_4) \equiv \mathrm{Tr}\ [\hat{V}(\tau_1)\ \hat{V}(\tau_2)\ \hat{V}(\tau_3)\ \hat{V}(\tau_4)\rho_a] \qquad \text{(VII-4a)}$$

where

$$\hat{V}(\tau) = \exp(iH\tau)\hat{V}\exp(-iH\tau) \qquad \text{(VII-4b)}$$

with $\hat{V}$ being the molecular electronic dipole operator given by

$$\hat{V} \equiv \mu[|a\rangle\langle b| + |b\rangle\langle a|] \qquad \text{(VII-4c)}$$

and the Hamiltonian H is given by eq II-2. We also have

$$|\mu|^2 J(t) = \mathrm{Tr}\ [\hat{V}(t)\ \hat{V}(0)\rho_a] \qquad \text{(VII-5)}$$

It is hard to develop physical intuition and useful approximations for eq VII-3. In the Liouville space, we follow naturally the actual sequence of events (a certain propagation for the interval t_1, followed by the interval t_2 and by t_3). In eq VII-3, all the time arguments are mixed. Equations II-13, on the other hand, which are based on calculating the generating function in Liouville space rather than the wave function in Hilbert space, provide a natural framework for developing a semiclassical picture of solvation.

Let us discuss the response functions in more detail. $J(t_1)$ represents the transition from $\hat{\rho}_{aa}$ (denoted aa) to $\hat{\rho}_{bb}$ (denoted bb) in second order. As seen in Figure 1 (pathway labeled A), we start with $\hat{\rho}_{aa}$ and apply one interaction from the left going to $\hat{\rho}_{ba}$, and then a second interaction from the right leads to bb. Another pathway which leads from $\hat{\rho}_{aa}$ to $\hat{\rho}_{bb}$ in second-order runs through $\hat{\rho}_{ab}$ (first interaction from the right and second from the left). This pathway gives $J^*(t_1)$. The total linear response function is $[J(t_1) - J^*(t_1)]$. In spectroscopy $\hat{\rho}_{ab}$ or $\hat{\rho}_{ba}$ denotes an optical coherence and the linear response function is related to the absorption line shape. In rate processes, $\hat{\rho}_{ab}$ is the transition state for the rate process. $iV(\hat{\rho}_{ba} - \hat{\rho}_{ab})$ is the flux for the a to b transition.[12]

In Figure 1B, we display four pathways leading from aa to bb in fourth order. These pathways constitute $R(t_3,t_2,t_1)$. There are four additional pathways whose contribution is the complex conjugate of the former. The third-order nonlinear response function is $[R(t_3,t_2,t_1) - R^*(t_3,t_2,t_1)]$.

Let us have a closer examination of the physical significance of these pathways in rate process. Pathways i and ii (R_1 and R_2) pass through an intermediate state $\hat{\rho}_{bb}$ after two interactions. At that point the reactant changed into the product but the solvation coordinate U is not in thermal equilibrium with respect to the Hamiltonian H_b. It then undergoes relaxation to equilibrium. When it reaches equilibrium $R_\alpha(t_3,t_2,t_1) = R_\alpha(t_3,\infty,t_1)$, and this pathway does not contribute to the reaction rate any more (see eq II-26b). It will be shown below that the time scale for this equilibrium process is $\tau[(E^\circ - \lambda)/\Delta]$. Pathways iii and iv ($R_3$ and R_4) pass through an intermediate state $\hat{\rho}_{aa}$ after two interactions. This represents processes in which the system passed through the transition state and returned back to a. Again, the solvation coordinate for the molecules undergoing this process is not in thermal equilibrium with respect to H_a, and it relaxes to equilibrium in a time scale $\tau[(E^\circ + \lambda)/\Delta]$, as will be shown below. When this relaxation is completed, these pathways do not contribute to the rate since $R_\alpha(t_3,t_2,t_1) = R_\alpha(t_3,\infty,t_1)$ (see eq II-26b).

We are now in a position to discuss the physical significance of the solvent time scale function $\tau(z)$. To that end we need to introduce a few definitions. We denote by $S_m(x)$ the probability density of the solvation coordinate U (eq III-10) to have the value x, when the system is in the state m

$$S_m(x) \equiv \langle\delta(x - U)\rho_m\rangle \qquad m = a, b \qquad \text{(VII-6)}$$

We further define the *conditional probability* for the solvation coordinate U to have the value x at time t, given that it had the value y at $t = 0$ and that the system is in the state m

$$W_m(x,t;y) \equiv S_a^{-1}(y)\langle\delta[x - U_m(t)]\delta(y - U)\rho_a\rangle \qquad \text{(VII-7a)}$$

with

$$U_m(t) \equiv \exp(iH_m t)U\exp(-iH_m t) \qquad m = a,b \qquad \text{(VII-7b)}$$

As $t \to \infty$, we have

$$W_m(x,t\to\infty;y) = S_m(x) \qquad \text{(VII-7c)}$$

We have shown that $\tau[(E^\circ - \lambda)/\Delta]$ came from pathways i and ii and $\tau[(E^\circ + \lambda)/\Delta]$ came from pathways iii and iv. They are given by[46]

$$\tau\left(\frac{E^\circ - \lambda}{\Delta}\right) = (2\pi)^{1/2}\Delta\int_0^\infty dt\ [W_b(-E^\circ,t;-E^\circ) - S_b(-E^\circ)] \qquad \text{(VII-8a)}$$

$$\tau\left(\frac{E^\circ + \lambda}{\Delta}\right) = (2\pi)^{1/2}\Delta\int_0^\infty dt\ [W_a(-E^\circ,t;-E^\circ) - S_a(-E^\circ)] \qquad \text{(VII-8b)}$$

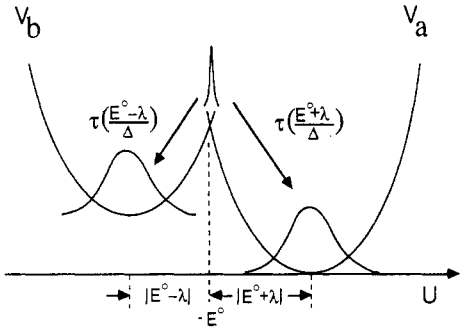

Figure 11. The dynamics underlying the solvent time scale function $\tau(z)$ (eq III-19 and VII-8). We start with a fluctuation of the solvation coordinate at the transition state (curve crossing) $U = -E^\circ$. If the system is in the $|a\rangle$ state (R_3 and R_4), this fluctuation will relax to $S_a(U)$ with a characteristic time scale $\tau[(E^\circ + \lambda)/\Delta]$. If the system is in the $|b\rangle$ state (R_1 and R_2), it will relax to $S_b(U)$ and the characteristic time scale is $\tau[(E^\circ - \lambda)/\Delta]$.

$\tau[(E^\circ - \lambda)/\Delta]$ is thus the average time it takes for a solvent fluctuation at the transition state ($U = -E^\circ$) to relax to thermal equilibrium in the state $|b\rangle$, whereas $\tau[(E^\circ + \lambda)/\Delta]$ is the average time it takes for the same fluctuation to relax to thermal equilibrium in the state $|a\rangle$. This is represented schematically in Figure 11. If these times are fast, the fourth-order contribution to the rate vanishes and the rate is adiabatic. The transition from the nonadiabatic to the adiabatic limit is therefore a result of the finite relaxation time of the solvent which results in a change of the distribution of the solvation coordinate U during the course of the rate process. It should be stressed that eq VII-8 were obtained by a careful evaluation of the nonlinear response functions. We did not have to assume a priori that the reaction takes place at the transition-state configuration $U = -E^\circ$.

It should further be noted that, in fluorescence measurements, the Stokes shift depends on solvent relaxation in the excited state (R_1 and R_2). In hole burning, we probe a difference between the ground and the excited states and therefore all pathways R_1, R_2, R_3, and R_4 contribute. Hole-burning spectroscopy is thus a probe for ground-state as well as excited-state relaxation.[42]

The present formulation is based on a generalized master equation, and we have derived a frequency-dependent rate $K(s)$. The s scale over which $K(s)$ varies is determined by the solvation time scales. The values of s, relevant in the generalized master equation, are approximately equal to the inverse reaction time scale (the rate). Reactions with large activation barriers are slow, and a separation of time scales is expected to hold, resulting in ordinary rate equations (eq II-22). For barrierless reactions this separation of time scales may not hold. Several optically induced electron-transfer and isomerization reactions show a time evolution which does not follow a simple rate equation.[8,30] Our generalized rate equation provides an adequate method for treating these reactions by keeping the s dependence of $K(s)$ and allowing for an initial nonequilibrium distribution of the solvation coordinate.

Acknowledgment. The support of the National Science Foundation, the Office of Naval Research, the U.S. Army Research Office, and the donors of the Petroleum Research Fund, administered by the American Chemical Society, is gratefully acknowledged.

ARTICLES

A Theoretical Study of the Interaction of Acetylene with Copper and Silver Monoions

Josefa Miralles-Sabater,† Manuela Merchán, Ignacio Nebot-Gil,* and Pedro M. Viruela-Martín

Departament de Química Física, Universitat de València, Dtor. Moliner 50, Burjassot, 46100, Valencia, Spain
(Received: July 13, 1987)

The interaction of copper and silver monoions with acetylene has been studied including the effect of electron correlation. Geometries of the minima and binding energies have been determined by using properly localized molecular orbitals in the configuration interaction. Although the main interaction is due to the presence of a positive charge, inclusion of electron correlation is needed if accurate results are desired. In the light of the present results, and considering previous works on metal–ligand bonding, the validity of the two-way donor–acceptor model is analyzed.

Introduction

The model proposed by Dewar[1] in 1951 to explain the bonding in π-coordinated metal–olefin complexes has been considered as a useful scheme to rationalize this type of bonding.[2] The interaction between an olefin and a metal located above the ligand molecular plane and equidistant from the two carbon atoms is attributed by Dewar's model to the two-way donor–acceptor interaction. On the one hand, σ-bonding charge donation takes place from ligand to metal and, on the other hand, π-bonding back-donation of metal electrons to the ligand (σ and π referring to rotational symmetry of the orbitals implied). In 1953 the "π-complex theory of metal–olefin complexes"[3] was first applied by Chatt and Duncanson[4] to explain the nature of the chemical bond in platinum–olefin complexes. After that, great efforts have been devoted to analyze the metal–ligand bond in terms of σ- and π-bonding. It is worthwhile to recall that the metal–ligand interactions are involved in many fields of current chemical research. The study of such complexes may produce some insight into relevant aspects of homogeneous and heterogeneous catalysis,

† Present address: Departament de Química, Facultat de Químiques de Tarragona, Pl. Imperial Tarraco No. 1, 43005 Tarragona, Spain.

(1) Dewar, M. J. S. *Bull. Soc. Chim. Fr.* **1951**, *18*, C71.
(2) Cotton, F. A.; Wilkinson, G. *Advanced Inorganic Chemistry*, 3rd. ed.; Wiley: New York, 1972.
(3) See comments in: Dewar, M. J. S.; Ford, G. P. *J. Am. Chem. Soc.* **1979**, *101*, 783.
(4) Chatt, J.; Duncanson, L. A. *J. Chem. Soc.* **1953**, 2939.

0022-3654/88/2092-4853$01.50/0